Dynamical-system formulation of the eigenvalue moment method

C. R. Handy
Department of Physics, Clark Atlanta University, Atlanta, Georgia 30314

B. G. Giraud and D. Bessis
Service de Physique Theorique, Centre d'Etudes Nucléaires, Saclay, F-91190 Gif-sur-Yvette, France
(Received 22 January 1991)

The eigenvalue moment method (EMM), a linear-programming (LP) based technique for generating converging bounds to quantum eigenenergies, is reformulated as an iterative dynamical system (DS). Important convexity properties are uncovered significantly impacting the theoretical and computational implementation of the EMM program. In particular, whereas the LP-based EMM formulation (LP-EMM) can require the generation and storage of many inequalities [up to several thousand for a 10-missing moment problem ($m_s=10$)], the dynamical-system formulation (DS-EMM) generates a reduced set of inequalities [of order $O(m_s+1)$]. This is made possible by replacing the LP generation of *deep interior points* (DIP's) by a Newton iteration process. The latter generates an optimal set of DIP's sufficient to determine the existence or nonexistence of the relevant *missing moment* polytopes. The general DS-EMM theory is presented together with numerical examples.

INTRODUCTION

The development of bounding methods for calculating eigenenergy spectra has been an important theoretical problem for many decades [1]. These concerns become practically relevant in the analysis of singular, strongly coupled, quantum systems where traditional methods can give rise to significantly varying estimates [2]. In such cases, the availability of tight bounds allows one to determine the correct value and discriminate between competing theories.

The eigenvalue moment method (EMM) is one of the few bounding theories that can yield converging bounds to the low-lying spectrum of multidimensional Hamiltonians. The analysis of arbitrary excited states is also possible through the recently developed C-shift formulation [3]. Although important theoretical and computational advances have been achieved through EMM, its present algorithmic structure may prove impractical in the analysis of few-body problems. These issues are the focus of this paper and subsequent works which are dedicated to improved theoretical analysis impacting the algorithmic implementation of the EMM theory.

Previous formulations of EMM [2,4] made heavy use of linear-programming (LP) theory [5] in order to determine the existence of certain important nonlinear convex sets. This presented an important breakthrough in comparison to earlier attempts which directly analyzed nonlinear Hankel-Hadamard determinantal inequality constraints [6]. Nevertheless, the LP-based EMM formulation (LP-EMM) requires the computer storage of many inequalities. For the two space dimension quadratic Zeeman problem [2], involving up to $m_s=10$ independent variables (missing moments), several thousand inequalities had to be stored for each energy parameter value examined. We consider this to be a serious impediment in the analysis of larger systems (potentially) involving hundreds of independent variables [$m_s=O(10^2)$] and many thousands of inequalities.

In principle, one can reduce the number of inequalities that must be stored to only $2m_s$. Specifically, as was done in Ref. [4], one can repeatedly find the extremal vertices for each generated polytope and thereby define a circumscribing hyperrectangular polytope. This process is not too efficient since the latter may be much larger than the original polytope. Nevertheless, the computer storage demands would be reduced.

A more efficient approach is that offered by a dynamical-system reformulation. Indeed, this achieves the same objectives defined above and also allows for parallel processing (refer to Sec. II B). In addition, important convexity properties are uncovered that significantly enhance our understanding of the basic EMM theory itself.

In Sec. I we review the LP-EMM formulation so as to better appreciate the dynamical-system approach (DM-EMM) presented in Sec. II. Included are applications of the DS-EMM analysis with respect to the quartic potential and the sextic anharmonic oscillator. Important derivations are left to the appendixes.

I. LINEAR PROGRAMMING EIGENVALUE MOMENT METHOD (LP-EMM)

The basic philosophy of the EMM theory is to transform the Schrödinger equation into a *moment problem* representation in which the physical solution is "uniquely" associated with an asymptotically bounded and nonnegative configuration. Explicitly, this involves defining a linear recursion moment equation, where the energy E appears as a parameter and the independent-initialization moments $\{u(i)|\ 0\le i\le m_s\}$ (for one space dimension) are

referred to as missing moments. Upon imposing an appropriate normalization constraint, the missing moments can be restricted to lie within the unit hypercube: $\{0<u(i)<1 \mid 1\le i\le m_s\}$. The latter is referred to as the initialization polytope (a polytope is a convex set defined by intersecting hyperplanes).

Since the desired eigenstate is uniquely representable by a bounded and non-negative wave function, the classic moment problem [7] defines an infinite hierarchy of additional constraints by which to further restrict the admissible missing moment solution set. These constraints appear in the form of nonlinear Hankel-Hadamard (HH) determinantal inequalities. Up to a given (HH) order, for an arbitrary E value, if the missing moment constraints admit a solution set $\mathcal{C}(E)$, then it must be convex. The major objective of any EMM analysis is to determine the existence or nonexistence of $\mathcal{C}(E)$, for each E. The E values for which $\mathcal{C}(E)$ exists define the admissible set (i.e., lower and upper bounds) of energy values within which lies the true physical energy. As the order of the calculation increases, the eigenenergy bounds become progressively tighter, converging to the physical value.

The traditional algorithmic implementation of the EMM theory uses linear programming in order to determine the existence or nonexistence of $\mathcal{C}(E)$ [2,4]. For each E value chosen, the initialization polytope is repeatedly "cut up" by determining at each step (1) a deep interior point (DIP) to the (updated) polytope; and (2) finding all the appropriate hyperplanes, at the corresponding DIP, that intersect the polytope; thus generating a smaller polytope. This "cutting" process is iterated many times until either no "cutting" vectors (intersecting hyperplanes) are found or no polytope remains; thereby establishing the existence or nonexistence of $\mathcal{C}(E)$, respectively. To facilitate the overall presentation, we outline the structure of the LP-EMM approach in the context of the sextic anharmonic oscillator problem defined below.

A. LP-EMM analysis of the sextic anharmonic oscillator

Consider the sextic anharmonic oscillator problem

$$-\Psi''(x)+(mx^2+gx^6)\Psi(x)=E\Psi(x)\ , \tag{1.1}$$

where E, m, and g correspond to the energy, mass, and coupling strength, respectively. For simplicity, we limit this discussion to the analysis of the ground state which is known to correspond to a non-negative wave function [8].

Applying $\int_{-\infty}^{\infty} dx\, x^q$ to both sides of Eq. (1.1) and performing the necessary integration by parts, one generates a recursion relation for the Hamburger moments $\mu(q)=\int_{-\infty}^{\infty} dx\, x^q\Psi(x)$:

$$\mu(q+6)=[E\mu(q)-m\mu(q+2)+q(q-1)\mu(q-2)]/g\ . \tag{1.2}$$

The underlying symmetry can be exploited by directly working within a Stieltjes moment representation effectuated through the change of variables, $y=x^2$, with associated moments $u(p)=\mu(2p)=\int_0^{\infty} dy\, y^p\Psi(\sqrt{y})/\sqrt{y}$, $p\ge 0$. The corresponding Stieltjes moment recursion relation is

$$u(p+3)=[Eu(p)-mu(p+1)+2p(2p-1)u(p-1)]/g\ . \tag{1.3}$$

The energy appears as a parameter. Three initialization variables $\{u(0),u(1),u(2)\}$ must be specified before all other moments can be determined. We refer to these as missing moments. The homogeneous character of the Schrödinger equation is also apparent in Eq. (1.3), allowing the imposition of any convenient normalization prescription. One such choice is

$$u(0)+u(1)+u(2)=1\ , \tag{1.4}$$

which is used to eliminate $u(0)$. This, combined with the non-negativity of the ground-state wave function restrict $u(1)$ and $u(2)$ to the unit square.

The structure of Eq. (1.3) can be equivalently represented in terms of

$$u(p)=\sum_{l=0}^{m_s} M(E;p,l)u(l)\ , \tag{1.5}$$

where $m_s=2$, and the energy-dependent coefficients $M(E;p,l)$ satisfy the same recursion relation in Eq. (1.3) with respect to the index p. In addition, they must also satisfy the conditions

$$M(E;i,j)=\delta_{i,j} \quad \text{for } i,j=0,1,\ldots,m_s\ . \tag{1.6}$$

In terms of the unconstrained missing moments $\{u(1),u(2)\}$ we have

$$u(p)=\sum_{l=0}^{m_s} \hat{M}(E;p,l)\hat{u}(l)\ , \tag{1.7a}$$

where

$$\hat{M}(E;p,l)=\begin{cases} M(E;p,l)-M(E;p,0) & \text{for } l=1,\ldots,m_s \\ M(E;p,0) & \text{for } l=0\ , \end{cases} \tag{1.7b}$$

and

$$\hat{u}(p)=\begin{cases} u(p) & \text{if } p>0 \\ 1 & \text{if } p=0\ . \end{cases} \tag{1.7c}$$

The classic theory of the moment problem tells us that the necessary and sufficient conditions for a set of Stieltjes moments $\{u(p)\}$ to be the moments of a non-negative function are that the Hankel-Hadamard determinants be positive. That is,

$$\Delta_{m,n}\{u\}>0 \text{ for } m=0,1 \text{ and } n=0,1,\ldots, \tag{1.8a}$$

where

$$\Delta_{m,n}\{u\}=\mathrm{Det}\begin{bmatrix} u(m) & u(m+1) & \cdots & u(m+n) \\ u(m+1) & u(m+2) & & u(m+n+1) \\ \vdots & & & \vdots \\ u(m+n) & u(m+n+1) & \cdots & u(m+2n) \end{bmatrix} . \tag{1.8b}$$

We shall use the notation $\mathcal{M}_{m,n}[u]$ to symbolize the Hankel matrix appearing in Eq. (1.8b). Note that the maximum moment order contributing to an HH determinant is $m+2n$. If $\mathcal{P}$ is the maximum moment order generated from the moment recursion relation, then only those matrices satisfying $m+2n \le \mathcal{P}$ are relevant. Given m (0 or 1), the largest n-order is the largest integer n_m satisfying $n_m \le (\mathcal{P}-m)/2$.

Each of the inequality relations in Eq. (1.8a) defines, through Eqs. (1.7), a nonlinear inequality constraint on the missing moments $u(1)$ and $u(2)$. For a given energy parameter value E and maximum moment order $\mathcal{P}$, one must determine if the corresponding set of HH inequalities admits a missing moment solution set, $\mathcal{C}(E)$. If it exists, then, as previously indicated, it must be convex.

The adopted missing moment normalization, together with the non-negativity of the physical ground-state configuration, restricts $\mathcal{C}(E)$ to lie within the unit square. Actually, because of Eq. (1.4), and the requirement that $u(0)>0$, $\mathcal{C}(E)$ must lie within the triangle defined by $0<u(1)<1$, $0<u(2)<1$, and $u(1)+u(2)<1$. However, the latter is contained in the HH inequalities (i.e., $\Delta_{0,0}$); consequently, the initialization polytope is the unit square.

Clearly, to work with the HH determinants is inconvenient, particularly when problems with a large number of missing moments are considered. Fortunately, the LP-EMM approach makes use of a fundamental linearization of the HH inequalities.

It is well known [7] that an equivalent linear formulation of Eq. (1.8) is defined by the inequality constraints

$$\langle \tilde{C}|\mathcal{M}_{m,n}[u]|\tilde{C}\rangle > 0 \quad \text{for } m=0,1, \quad n=0,1,\ldots, \tag{1.9a}$$

and arbitrary (nonzero) $\tilde{C}$ vectors (of implicit dimension $n+1$); alternatively

$$\min_{m=0,1}\{\langle \mathcal{V}_{m,n}|\mathcal{M}_{m,n}[u]|\mathcal{V}_{m,n}\rangle\} > 0 \quad \text{for } n=0,1,\ldots, \tag{1.9b}$$

where $\mathcal{V}_{m,n}$ is the normalized eigenvector for the smallest eigenvalue of the indicated Hankel matrix (hereafter, $\mathcal{V}$ will have this connotation).

If the nonlinear convex set $\mathcal{C}(E)$ exists, it may be equivalently defined in terms of an infinite envelope of circumscribing straight lines (hyperplanes). Therefore we may think of Eq. (1.9a) as defining $\tilde{C}$ vectors which generate cuttings in the missing moment space that cut up the initialization polytope (the unit square) down to $\mathcal{C}(E)$. If $\mathcal{C}(E)$ does not exist, one can find an optimal set of cuttings that quickly cut up the initialization polytope into the null set, thereby confirming the nonexistence of $\mathcal{C}(E)$. This is the essence of the LP-EMM approach. We proceed to describe the technical structure of the "cutting method."

B. LP-EMM cutting procedure

We now proceed to describe the iterative process by which the unit square is cut up in order to determine $\mathcal{C}(E)$'s existence or nonexistence. The following discussion is phrased in general terms. It is implicitly understood that the starting polytope is the associated unit square (or more generally, unit hypercube). For further details consult Refs. [2] and [4].

Step 1. Firstly, linear-programming methods are used to find the largest inscribed circle (hypersphere) to a given polytope, $\mathfrak{P}_\tau$. The center of this circle defines a deep interior point (DIP) to $\mathfrak{P}_\tau$.

Step 2. Secondly, at the DIP point, $(u_\alpha(1), u_\alpha(2))$, the largest Hankel matrices $\mathcal{M}_{m,n_m}[u_\alpha]$, consistent with the maximum moment order $\mathcal{P}$, are analyzed to determine if suitable cuttings exist which can be used to reduce $\mathfrak{P}_\tau$ into a smaller polytope $\mathfrak{P}_\tau^*$. If cuttings exist, then step 1 is repeated with respect to $\mathfrak{P}_\tau^*$. The iterative process continues until either no further cuttings are possible, or the remaining polytope is the null set, thereby affirming that $\mathcal{C}(E)$ does or does not exist, respectively.

With regards to step 2 the process of identifying suitable cutting vectors is as follows. Let λ denote the smallest eigenvalue of the set of eigenvalues for both Hankel matrices:

$$\lambda = \min_{m=0,1}\{\text{eigenvalues of } \mathcal{M}_{m,n_m}[u_\alpha]\} . \tag{1.10}$$

The particular $\mathcal{M}_{m,n_m}$ for which λ is an eigenvalue will be referred to as $\mathcal{M}_\alpha$ (i.e., the corresponding m and n_m are denoted by m_α and n_α, respectively).

If λ is nonpositive,

$$\lambda \le 0 , \tag{1.11}$$

then its associated eigenvector $\mathcal{V}_\alpha$ will generate a "cut" on $\mathfrak{P}_\tau$, resulting in a smaller polytope $\mathfrak{P}_\tau^*$ (which could also be the null set). If λ is positive, no cutting is said to be generated. Actually, in this case, $\mathcal{V}_\alpha$ may still generate a cut on the initialization polytope; however, once a positive λ is found, $\mathcal{C}(E)$'s existence is affirmed and we may then proceed to a different E value.

In order to understand all the above, consider the $\mathcal{V}_\alpha$

generated line (hyperplane) in the $u_1 \times u_2$ missing moment space [$u_1 = u(1)$, $u_2 = u(2)$, $m_s = 2$]:

$$\mathcal{L}_d[u_1, u_2] = 0 \ , \tag{1.12a}$$

where

$$\mathcal{L}_d[u_1, u_2] = \sum_{l=0}^{m_s} \langle (\mathcal{V}_d)_i | \hat{M}(E; m_d + i + j, l) | (\mathcal{V}_d)_j \rangle \hat{u}_l \ . \tag{1.12b}$$

Note that $(\mathcal{V}_d)_i$ denotes the ith component of eigenvector $\mathcal{V}_d$. All repeated i,j indices are implied summations consistent with the associated expansion order $\mathcal{P}$ (i.e., $0 \le i,j \le n_d$).

The line defined by Eq. (1.12) divides the entire missing moment space in two, corresponding to the domains on which $\mathcal{L}_d[u]$ is nonpositive or positive. These are denoted by $\mathcal{H}_d^n$ and $\mathcal{H}_d^p$, respectively. If λ is nonpositive, then the DIP point $\mathbf{u}_d$ lies in $\mathcal{H}_d^n$. We assume this to be the case.

From Eq. (1.9), all of $\mathcal{H}_d^n$ contradicts the moment problem constraints. That is, for $u \in \mathcal{H}_d^n$, the Hankel matrix $\mathcal{M}_d[u]$ invalidates Eq. (1.9) because we can take $\tilde{C}$ to be $\mathcal{V}_d$ (i.e., $\langle \mathcal{V}_d | \mathcal{M}_d[u] | \mathcal{V}_d \rangle \le 0$ if $u \in \mathcal{H}_d^n$). Accordingly, if $\mathcal{C}(E)$ exists, it must lie within $\mathcal{H}_d^p$. Through $\mathcal{H}_d^p$ we can cut the polytope $\mathfrak{P}_\tau$ into a smaller polytope $\mathfrak{P}_\tau^* = \mathfrak{P}_\tau \cap \mathcal{H}_d^p$.

The entire process is repeated with respect to $\mathfrak{P}_\tau^*$ until either no cutting vectors can be found ($\lambda > 0$) or no polytope remains (i.e., the null set). These correspond to establishing that $\mathcal{C}(E)$ either exists (to moment order $\mathcal{P}$) or does not exist, respectively.

In Fig. 1 we illustrate a symbolic sequence of DIP points and their corresponding cutting lines, as defined by Eq. (1.12). For a given DIP point $\mathbf{u}_d$, the closest point $\mathbf{u}_c$ on its corresponding cutting line, $\mathcal{L}_d(u) = 0$, is given by

$$u_{c_l} = u_{d_l} - \frac{\sum_{l'=0}^{m_s} \langle (\mathcal{V}_d)_i | \hat{M}(E; m_d + i + j, l') | (\mathcal{V}_d)_j \rangle \hat{u}_{d_{l'}}}{\sum_{l'=1}^{m_s} \langle (\mathcal{V}_d)_i | \hat{M}(E; m_d + i + j, l') | (\mathcal{V}_d)_j \rangle^2} A_l \ , \tag{1.13a}$$

where $A_l = \langle \mathcal{V}_d | \hat{M}(E; m_d + \cdots, l) | \mathcal{V}_d \rangle$ and $1 \le l \le m_s$ (the ellipses denote implicit indicial summations). Alternatively we may rewrite the above as

$$\mathbf{u}_c = \mathbf{u}_d - \frac{\langle \mathcal{V}_d | \hat{\mathcal{M}}_d[u_d] | \mathcal{V}_d \rangle}{\sum_{l=1}^{m_s} \langle (\mathcal{V}_d)_i | \hat{M}(E; m_d + i + j, l) | (\mathcal{V}_d)_j \rangle^2} \mathbf{A} \ . \tag{1.13b}$$

Refer to Appendix A for a description of the relevant geometry.

Although $\mathcal{L}_d[\mathbf{u}_c] = \langle \mathcal{V}_d | \mathcal{M}_d[\mathbf{u}_c] | \mathcal{V}_d \rangle = 0$, the point $\mathbf{u}_c$ can also generate its own cutting line in a manner identical to that for $\mathbf{u}_d$. One can then proceed to identify $\mathbf{u}_c$'s closest point on its associated cutting line. This process can be iterated indefinitely, resulting in the sequence of points symbolically depicted in Fig. 2. Numerical experimentation with such sequences revealed them to be globally stable and convergent to the boundary of $\mathcal{C}(E)$, when the latter exists. This behavior suggested a deeper convex-function structure than that already discussed, leading to the DS-EMM formulation presented in Sec. II.

The DS-EMM formalism in Sec. II will show that the

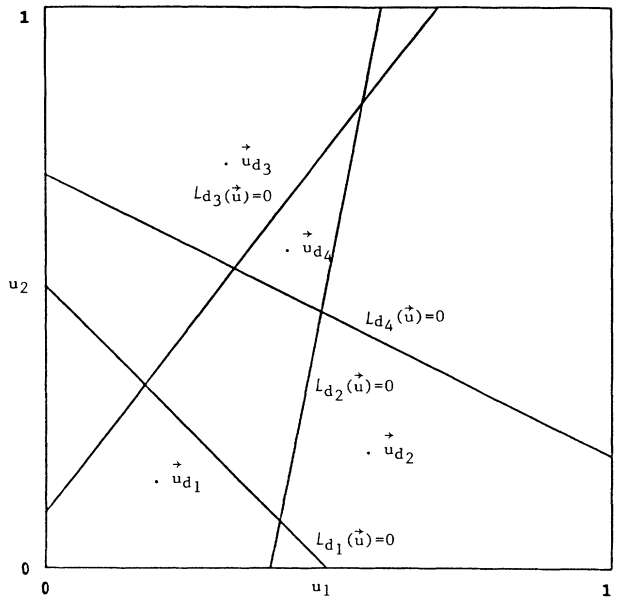

FIG. 1. Symbolic sequence of DIP points and their cutting lines, $\mathcal{L}_{d_i}(\mathbf{u}) = 0$.

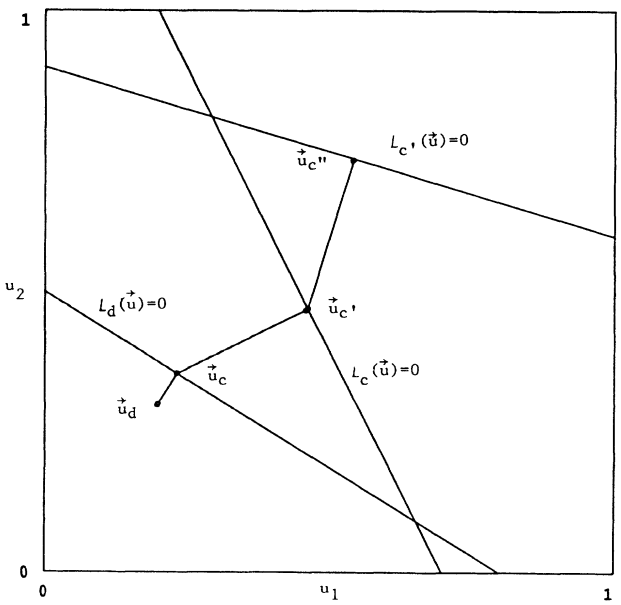

FIG. 2. Symbolic sequence of Newton iteration points and associated cutting lines.

iterates depicted in Fig. 2 correspond to the Newton-iteration points of the convex (spline) function

$$F[\mathbf{u}]=\min_{m=0,1}\{\langle \mathcal{V}[\mathbf{u}]|\mathcal{M}_{m,n_m}[\mathbf{u}]|\mathcal{V}[\mathbf{u}]\rangle\}\ , \tag{1.14}$$

where once again $\mathcal{V}[\mathbf{u}]$ is the eigenvector for the smallest eigenvalue of the indicated matrix and n_m is the largest index consistent with the maximum moment order generated, $\mathcal{P}$.

If $\mathcal{C}(E)$ exists, then the Newton iterates $\{\mathbf{u}_i\}$ may define a converging sequence $\{(\mathbf{u}_i,F[\mathbf{u}_i])\}$. If $\mathcal{C}(E)$ does not exist, the associated sequence of points $\{(\mathbf{u}_i,F[\mathbf{u}_i])\}$ will be nonconvergent and oscillatory. Conversely, these properties can be exploited to quickly determine if $\mathcal{C}(E)$ exists or not.

II. A DYNAMICAL-SYSTEM FORMULATION OF THE EMM THEORY (DS-EMM)

We present the dynamical-system formulation of the EMM theory (DS-EMM) by way of the one space dimension problems: the quartic potential and the sextic anharmonic oscillator. The generalization to higher-dimensional problems (both spatially and with respect to the missing moment order, m_s) proceeds identically to these lower-dimensional problems. In the interest of simplicity of presentation, we limit the analysis to the ground-state eigenvalue, for which the associated wave function is bounded and positive. Interspersed within the discussion on the quartic potential are the necessary generalizations for implementing the DS-EMM analysis with respect to the general missing moment problem; however, no explicit vector notation is used.

A. Quartic potential problem and appropriate generalizations

Consider the quartic potential problem

$$-\Psi''(x)+x^4\Psi(x)=E\Psi(x)\ . \tag{2.1}$$

The corresponding Stieltjes moment equation is

$$u(p+2)=Eu(p)+2p(2p-1)u(p-1)\ . \tag{2.2}$$

The missing moments are $u(0)$ and $u(1)$; however, upon adopting the normalization condition $u(0)+u(1)=1$ we obtain the analogous representation to that in Eqs. (1.5)–(1.7) with $m_s=1$:

$$u(p)=\sum_{l=0}^{m_s}\hat{M}(E;p,l)\hat{u}(l)\ , \tag{2.3}$$

where $\hat{M}(E;p,l)=M(E;p,l)-M(E;p,0)(1-\delta_{l,0})$, $\hat{u}(0)=1$, and $\hat{u}(1)=u(1)$. The unconstrained missing moment, $u(1)$, is restricted to the unit interval.

Let $\mathcal{P}$ correspond to the maximum order of generated moments [i.e., $u(0),u(1),\ldots,u(\mathcal{P})$]. As argued in Sec. I [refer to Eq. (1.9b)], a given energy parameter value E is a possible physical value, to order $\mathcal{P}$, if the function

$$F[E;u]=\min_{m=0,1}\{\langle \mathcal{V}_{m,n_m}[E;u]|\mathcal{M}_{m,n_m}[E;u]|\mathcal{V}_{m,n_m}[E;u]\rangle\}\ , \tag{2.4}$$

takes on positive values within the unit hypercube defined by the initialization polytope [i.e., the unit interval, $0<u(1)<1$, in the quartic case]. The subscript n_m is the largest integer satisfying $n_m\le(\mathcal{P}-m)/2$, for given m. The particular m and n_m values that define $F[E;u]$ at u are denoted by m_u and n_u, respectively. As indicated in Sec. I, the corresponding u-solution set (that on which F is positive) must be convex (i.e., an open interval in the $m_s=1$ quartic case). Occasionally, for clarity of presentation, we will omit $F[E;u]$'s explicit E dependence and refer to it as $F[u]$, a function of the unconstrained missing moment(s).

Let $\mathcal{C}(E)$ denote the missing moment set on which $F[E;u]$ is positive. It is possible that $\mathcal{C}(E)$ exists but does not intersect the initialization polytope. In such cases, the corresponding E value is unacceptable. Such situations are not expected to be as common as those for which $\mathcal{C}(E)$ does not exist all (i.e., $F[E;u]$ is nonpositive everywhere in the u space).

An important result that facilitates the determination of $\mathcal{C}(E)$ is as follows: The expectation values

$$F_{mn}[E;u_1,\ldots,u_{m_s}]=\langle \mathcal{V}_{m,n}[E;u]|\mathcal{M}_{m,n}[E;u]|\mathcal{V}_{m,n}[E;u]\rangle \tag{2.5}$$

are convex functions of the (unconstrained) missing moments $\{u_1,\ldots,u_{m_s}\}$, for any fixed and arbitrary E value. The proof is presented in Appendix B. From this it trivially follows that $F[E;u]$ must also be convex with respect to its missing moment dependence.

From $F[E;u]$'s definition, it is clear that it can (and will) be a continuous spline function differentiable almost everywhere. In the subsequent analysis, we assume that the Newton iterates do not lie at the nondifferentiable "spline" points. If by some (rare) chance an iterate point does coincide with a spline point, we can simply restart the iteration at a neighboring point where F is differentiable.

It is important to appreciate the significance of Eq. (1.12) in the present context. Let $(u,F[u])$ be a point in the space $\mathcal{U}\times\mathcal{F}$. The equation for the tangent hyperplane at $(u,F[u])$ is

$$\mathcal{F}=F[u]+(\alpha-u)\text{grad}F[u]\ . \tag{2.6}$$

The intersection of this tangent hyperplane with the missing moment plane ($\mathcal{F}=0$) defines the equation

$$\alpha A-B=0\ , \tag{2.7}$$

where $A=\text{grad}F[u]$ and $B=-(F[u]-u\ \text{grad}F[u])$. An important consequence of F's convexity is $F[\alpha]\leq\alpha A-B$, for all α.

The linear equation in α [Eq. (2.7)] defines a cutting of the missing moment space, as described in Sec. I. Let $\mathcal{H}_u^n$ and $\mathcal{H}_u^p$ denote the subsets (of the missing moment space) on which $\mathcal{L}[\alpha]=\alpha A-B$ is nonpositive and positive, respectively. From $F[\alpha]\leq\mathcal{L}[\alpha]$ it follows that the set $\mathcal{H}_u^n$ can be discarded; that is, if $\mathcal{C}(E)$ exists, it must lie within $\mathcal{H}_u^p$.

In summary, if at the point u we have $F[u]\leq 0$, then the intersection of the tangential hyperplane [Eq. (2.6)] with the missing moment subspace [Eq. (2.7)] defines a cutting of the unit hypercube (the initialization polytope); the good "side" is $\mathcal{H}_u^p$ and contains $\mathcal{C}(E)$, if the latter exists. The point u lies in $\mathcal{H}_u^n$.

In general, given a convex function, $F[u]$, a Newton iterated sequence will determine a zero point u_∞ ($F[u_\infty]=0$) if it exists. The general form for the Newton iteration is

$$u_{i+1}=u_i-F[u_i]\frac{\text{grad}F}{(\text{grad}F)^2}\ , \tag{2.8}$$

where (refer to Appendix B)

$$(\text{grad}F)_l=\langle\mathcal{V}[E;u]_i|\hat{M}(E;m+i+j,l)|\mathcal{V}[E;u]_j\rangle\ . \tag{2.9}$$

The $\mathcal{V}[E;u]$ expression in Eq. (2.9) is that which defines $F[E;u]$ in Eq. (2.4). The combination of Eqs. (2.8) and (2.9) and Eq. (2.4) is equivalent to Eqs. (1.13a) and (1.13b).

Returning to the quartic potential problem: if $\mathcal{C}(E)$ exists, then any Newton iteration sequence $\{u_i\}$ [i.e., $u(1)=u$] will converge to a point on the boundary, u_∞, corresponding to $F[E;u_\infty]=0$. In addition, the associated sequence $\{F[E;u_i]\}$ will also be convergent. In such cases, E's acceptability depends on whether or not u_∞ lies within the unit interval.

If $\mathcal{C}(E)$ does not exist, then the Newton iterates will be nonconvergent and oscillatory. Needless to say, in such cases E is unacceptable.

One cannot rely on the manifestation of convergence to decide if E is acceptable or not. This is because one does not know *a priori* how many iterations are necessary before convergence is established. Instead, several procedures are possible by which to determine, in a finite number of iteration steps, whether $\mathcal{C}(E)$ exists or not.

1. Establishing $\mathcal{C}(E)$'s existence

Confirmation of $\mathcal{C}(E)$'s existence is possible through two different approaches. The first of these involves the generation of a Newton sequence until convergence becomes manifest (i.e., the sequence differences $u_{i+1}-u_i$ become smaller than some tolerance). Assume that u_{i_c} is a sequence elements which we believe to be close to $\mathcal{C}(E)$'s boundary (and for which $F[E;u_{i_c}]$ is small in magnitude and negative). If so, then a gradient method could be used to locate a nearby point, u_*, lying within $\mathcal{C}(E)$ and satisfying $F[E;u_*]>0$. The identification of such a u_* point would confirm $\mathcal{C}(E)$'s existence.

A second approach for confirming $\mathcal{C}(E)$'s existence would involve the simultaneous generation of an arbitrary number, J, of Newton sequences $\{u_i^{(j)}\}$ ($1\leq j\leq J$ and $i=1,\ldots$). We assume that the initial points, $u_1^{(j)}$, are picked as far apart as possible so that the respective limits, $u_\infty^{(j)}$, correspond to (at least two) different points on $\mathcal{C}(E)$'s boundary. The convexity property guarantees that $(\sum_j u_\infty^{(j)})/J$ lies within $\mathcal{C}(E)$. It is therefore possible for the sequence of averages $\{u_i^{\text{av}}=(\sum_j u_i^{(j)})/J\}$ to lie within $\mathcal{C}(E)$ (that is, $F[E;u_i^{\text{av}}]>0$) before the iterates $\{u_i^{(j)}\}$ significantly converge to their respective $\mathcal{C}(E)$-boundary points. Numerical evidence of this would confirm the existence of $\mathcal{C}(E)$.

2. Establishing $\mathcal{C}(E)$'s nonexistence

The generation of eigenenergy bounds does not require knowing those E values for which $\mathcal{C}(E)$ exists. Instead, it is only necessary that one determine those E values for which $\mathcal{C}(E)$ does not exist. This is the approach adopted in this work.

An advantage provided by the DS-EMM approach over the LP-EMM formulation is that the nonexistence of $\mathcal{C}(E)$ can be readily confirmed through the identification of a very small number of DIP points, as generated by a Newton iteration scheme. For one-dimensional problems, $m_s=1$, these special DIP points are called saltation points, as explained below. Their multidimensional generalization ($m_s>1$), discussed in Sec. II B in the context of the sextic anharmonic oscillator, leads to an effective program for determining the nonexistence of $\mathcal{C}(E)$.

For the remainder of this discussion, as applied to the quartic problem, we will assume that the sole missing moment variable, $u(1)$, is denoted by α. In addition, $(\alpha,\mathcal{F})$ will refer to a point in the two-dimensional $\alpha\times\mathcal{F}$ space; while F will be used to refer to the function value $F[E;\alpha]$.

Consider the symbolic illustration in Fig. 3 depicting some sequential Newton iterates for the case where $\mathcal{C}(E)$ does not exist. At the u_i Newton iterate, the tangent line (hyperplane) equation is

$$\mathcal{F}=F[u_i]+(\alpha-u_i)\langle\mathcal{V}[u_i]|\hat{M}[m_i+\cdots,1]|\mathcal{V}[u_i]\rangle \tag{2.10}$$

[all notation is implicitly adopted from that in Eqs. (2.4) and (2.9)]. The associated α-space gradient vector is given by Eq. (2.9).

The α component of the point $(u_{\max},0)$ corresponds to the maximum of $F[\alpha]$. From $(u_{\max},0)$ we can draw two tangent lines to the F curve at points $\mathcal{S}_1=(u_{\mathcal{S}1},F_{\mathcal{S}1})$ and $\mathcal{S}_2=(u_{\mathcal{S}2},F_{\mathcal{S}2})$. We shall refer to points $\mathcal{S}_1$ and $\mathcal{S}_2$ as critical saltation points. Any iterate $(u_i,F[u_i])$ falling be-

tween the critical saltation points must generate an iterate on the "other side" of the $F[\alpha]$ curve. Any iterate lying within the critical saltation points shall be referred to as a saltation point. For one-dimensional missing moment problems, any u_i, which is also a saltation point, must satisfy

$$\text{grad}F[u_i]\text{grad}F[u_{i+1}]<0 \ . \tag{2.11}$$

One may also use Eq. (2.11) to define saltation points for multidimensional missing moment problems, $m_s>1$. In such cases, if u_i is a saltation point, then u_{i+1} lies on the other side of the one-dimensional F profile: $F[u_i+s\ \text{grad}\{F[u_i]\}]$, a function of the s variable.

It is readily appreciated from Fig. 3 that the tangent lines of any two successive saltation points (u_{i_1} and u_{i_2}) must circumscribe the convex set $\mathcal{C}_{\mathcal{F}}=\{(\alpha,\mathcal{F})|\mathcal{F}<F[\alpha]\}$ and negatively bound from above $F[\alpha]$ through their point of intersection, $F[\alpha]<\mathcal{F}_I<0$; thereby establishing the nonexistent of $\mathcal{C}(E)$.

Instead of identifying the intersection point in $\alpha\times\mathcal{F}$ for successive saltation-tangent lines, we may return to the LP-EMM perspective and identify for each saltation point its corresponding cutting of the initialization unit interval (unit hypercube), as described in the context of Eqs. (2.6) and (2.7). For the quartic case, the cuttings take place at the points defined by the intersection of the saltation tangent line with the α axis. When all the cuttings wipe out the unit interval, one concludes that $\mathcal{C}(E)$ does not exist. This cutting perspective is more convenient since it allows for the simultaneous use of an arbitrary number of saltation (and nonsaltation) -tangent lines.

The results of our analysis are quoted in Table I. The results are consistent with the LP-EMM analysis given in Ref. [6] (Handy and Bessis). The corresponding DS-EMM analysis (Table I) required only four (4) generated cutting inequalities (including the two corresponding to the unit interval constraint: $0<\alpha<1$), to all $\mathcal{P}$ orders, in determining nonexistent $\mathcal{C}(E)$'s, for E values outside of the bounds quoted in Table I. The maximum number of iterations was 40.

In Fig. 4 we simultaneously plot $F[E;\alpha]$ and some of the Newton iterates for the case $\mathcal{P}=6$ and $0.5\le E\le 1.5$. The admissible energy interval, to order $\mathcal{P}=6$, is (0.93,1.16). This is consistent with the true physical value 1.060 362 09 [9].

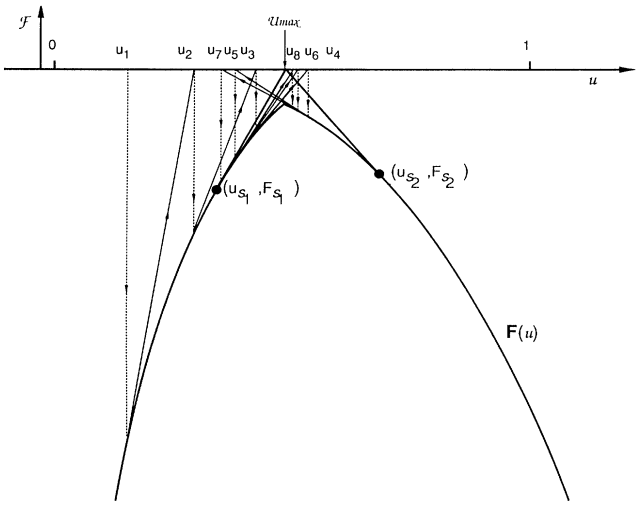

FIG. 3. Symbolic depiction of Newton iterates $\{u_i\}$ and saltation points $3\le i\le 8$.

B. Sextic anharmonic oscillator

All of the necessary equations and formulations for the sextic problem have been discussed in the previous sections. We dispense with repeating them and proceed to the relevant analysis concerning the identification of appropriate saltation points. The only reminder is that instead of dealing with a unit interval as the "initialization polytope" we are dealing with the unit square.

Geometrically, the multidimensional generalization of the results in Sec. II A makes saltation points of interest because only m_s+1 of them would be needed to determine the nonexistence of $\mathcal{C}(E)$. That is, the tangential hyperplanes of m_s+1 properly selected saltation points could circumscribe the convex set $\mathcal{C}_{\mathcal{F}}=\{(\alpha,\mathcal{F})|\mathcal{F}<F[\alpha]\}$, and (through the polytope defined by their intersection in the $\alpha\times\mathcal{F}$ space) negatively bound from above the maximum value of $F[\alpha]$.

In the $m_s=1$ case, the Newton iteration quickly generates appropriate saltation points by which to establish $\mathcal{C}(E)$'s nonexistence. Unfortunately, our experience with Newton iteration saltation points in the $m_s=2$ sextic case shows that little advantage is derived using them when compared to the LP-EMM approach. That is,

TABLE I. Newton iteration generated bounds for the quartic potential through the use of successive saltation points. The number of cuttings is four for each case (this number includes two cuttings due to unit interval specification constraints).

Max. I_{tr} [a]	Moment order $\mathcal{P}$	Energy bounds
40	6	$0.93<E<1.16$
40	7	$1.02<E<1.16$
40	8	$1.028<E<1.067$
40	9	$1.059<E<1.067$
40	10	$1.059<E<1.062\,0$
40	11	$1.059<E<1.061\,0$
40	12	$1.060\,2<E<1.061\,0$
40	13	$1.060\,2<E<1.060\,38$
40	14	$1.060\,34<E<1.060\,38$
40	15	$1.060\,353<E<1.060\,377$
40	16	$1.060\,353<E<1.060\,365$
40	17	$1.060\,361<E<1.060\,365$
40	18	$1.060\,361\,6<E<1.060\,362\,3$
40	19	$1.060\,361\,95<E<1.060\,362\,20$
40	20	$1.060\,362\,05<E<1.060\,362\,20$

[a] I_{tr} refers to the number of iterations.

there is no major reduction in the number of cutting inequalities that must be stored. The results quoted in Table II are the result of accepting successive saltation points provided the cuttings they generate in the missing moment space reduce the size of the polytope by a specified amount: $R_s(\mathfrak{P}_\tau^*)/R_s(\mathfrak{P}_\tau) \leq \epsilon_r$, where R_s is the radius of the largest circle inscribed within the polytope [4].

The results in Table II are due to the generation of a Newton iteration sequence, and the application of condition (2.11) in identifying all ensuing successive saltation points. Usually, the Newton iteration trajectory manifests a slowly evolving "almost-periodic" structure that may account for the large number of generated saltation points. That is, many of the saltation points are close to

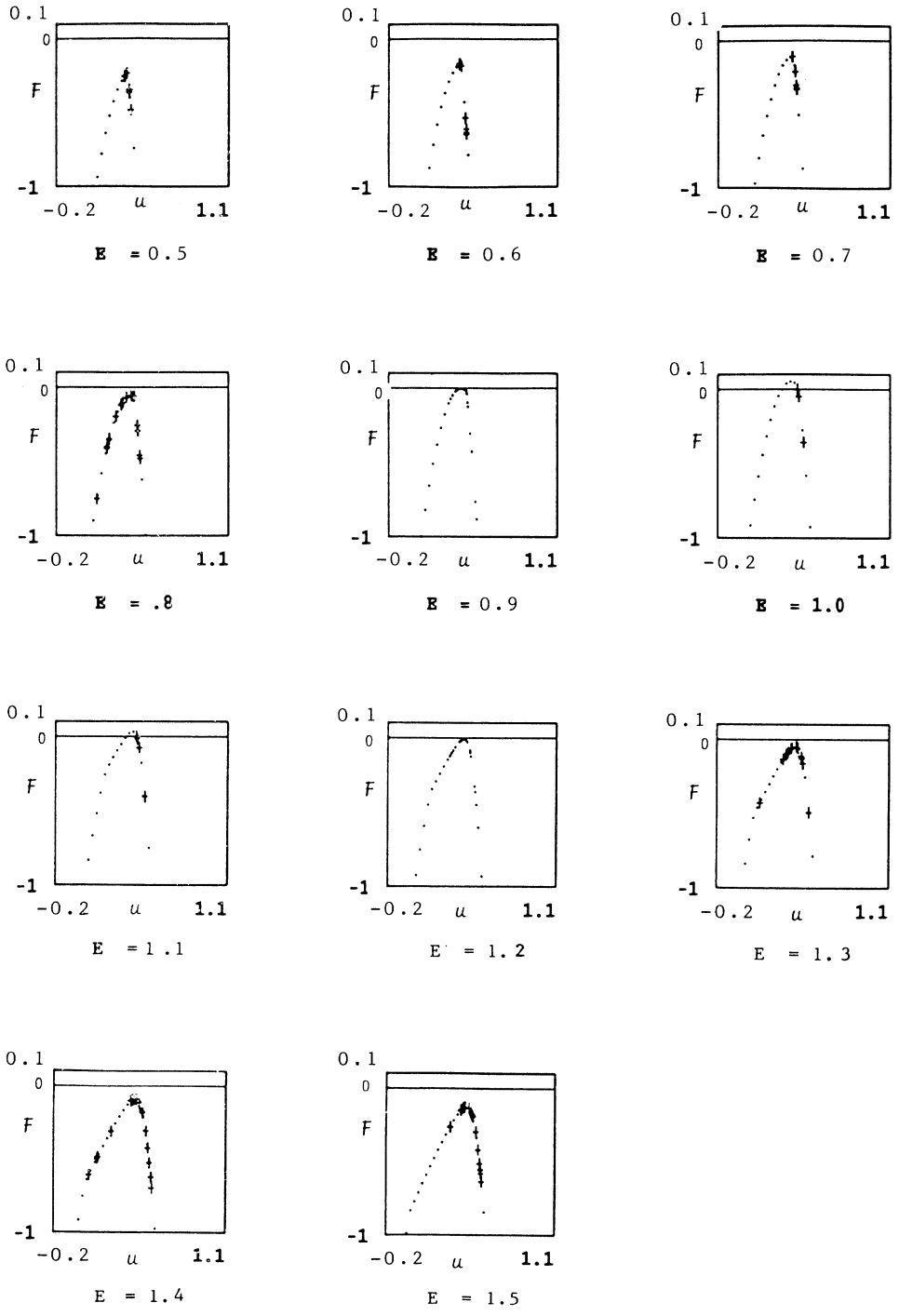

FIG. 4. Plot of $F[E;u]$ for the quartic potential, $\mathcal{P}=6$ (corresponding to dots) and some of the Newton iterates (+). The latter are depicted as dots in cases $E=0.9$ and 1.2 to avoid confusion.

TABLE II. Newton iteration determination of eigenenergy bounds for the sextic anharmonic oscillator ($m=g=1$) based upon identification of successive saltation points satisfying $R_s(\mathfrak{P}_\tau^*)/R_s(\mathfrak{P}_\tau)<f_r$.

No. of cuttings DS	LP [4]	f_r	Max. No I_{tr}	Moment order $\mathcal{P}$	DS-EMM ground-state energy bounds
8	20	0.9	60	8	$1.40<E<1.47$
10	25	0.7	60	10	$1.423<E<1.438$
9	35	0.7	60	12	$1.4352<E<1.4366$
17	43	0.9	60	14	$1.4354<E<1.4358$

each other; consequently, their associated cutting vectors contribute little to the total cutting of the unit square. Only when the Newton iteration trajectory makes a radical change will more effective saltation points be generated, significantly contributing to the total elimination of the unit square. In Fig. 5 we give an example of a typical Newton iteration trajectory.

Based upon the preceding results, a better strategy is to generate $2m_s$ different Newton iterates, $u_i^{(j)}$ $(1\le j\le 2m_s)$ by picking the $u_1^{(j)}$ starting elements as different as possible. For each iterate, the corresponding cutting inequality [Eqs. (2.6) and (2.7)] is generated:

$$\omega\cdot\mathcal{A}[u_i^{(j)}]-B[u_i^{(j)}]>0\ , \tag{2.12}$$

in addition to the unit square restriction $0<\omega_{1,2}<1$ (four inequalities in all). Note that $F[E;u_i^{(j)}]<0$, otherwise $\mathcal{C}(E)$ would be declared as existing.

At each iteration step (i), a simple application of linear programming is used to determine if the $2m_s$ inequalities (plus the four defining the unit square) admit a ω-solution set within the missing moment space. If at any iteration step there is no solution set, then $\mathcal{C}(E)$ does not exist, and the associated energy value E is declared unacceptable. In this manner, the energy bounds quoted in Table III were obtained. Note that only eight (8) inequalities are needed (including the four corresponding to the unit square), to arbitrary $\mathcal{P}$ order. Of course, the price one pays is that many iterations may be necessary.

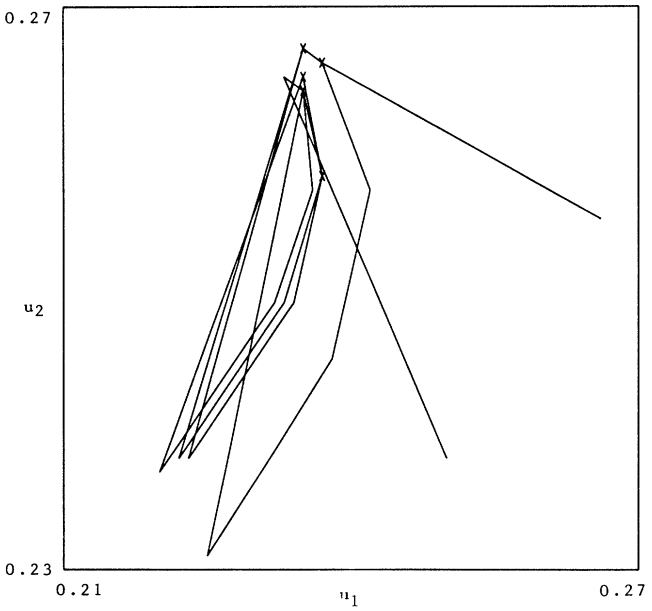

FIG. 5. Newton iterate trajectory for sextic anharmonic potential. The coincident saltation points (within the resolution depicted) are denoted by the cross symbols.

TABLE III. Obtaining ground-state energy bounds for the sextic anharmonic oscillator ($m=g=1$) by generating $2m_s=4$ Newton iterated sequences [corresponding to the initial points $u_1^{(1)}=(10,0)$, $u_1^{(2)}=(0,-10)$, $u_1^{(3)}=(-10,0)$, $u_1^{(4)}=(0,10)$]. The number of cutting inequalities is eight for all cases (this number includes the four inequalities corresponding to the unit square initialization polytope).

Max. No. of I_{tr}	$\mathcal{P}$	Ground-state energy bounds
15	8	$1.40<E<1.47$
30	10	$1.423<E<1.438$
25	12	$1.4352<E<1.4366$
70	14	$1.4354<E<1.4357$

It should be noted that the implementation of the above program is possible for any number $\mathcal{N}$ of simultaneous Newton iteration sequences provided $\mathcal{N}\ge m_s+1$. The minimum number of hyperplanes that can form a bounded polytope in an m_s-dimensional space is m_s+1. The greater $\mathcal{N}$ is, the faster (i.e., fewer number of iteration steps) the Newton iterated sequences can confirm the nonexistence of $\mathcal{C}(E)$. All of these issues are appropriate for parallel processing consideration.

CONCLUSION

A dynamical-system formulation for the eigenvalue moment method has been developed requiring the generation of fewer cuttings than that of the traditional LP-EMM theory discussed in Sec. I. This enables us to generate converging lower and upper bounds for the discrete spectrum of many quantum problems, including few-body systems such as the three-body problem (to be discussed in a subsequent paper).

ACKNOWLEDGMENTS

This work was supported through grants from the U.S. National Science Foundation and NATO (Grant No. 0427/88). Computer time was made available through a grant from the Pittsburgh Supercomputer Center. One of us (C.R.H.) acknowledges the hospitality of the Service de Physique Theorique of the Centre d' Etudes Nucléaires, Saclay, France. Finally, the computer technical support provided by Maribel Handy and Julian Niles is gratefully acknowledged.

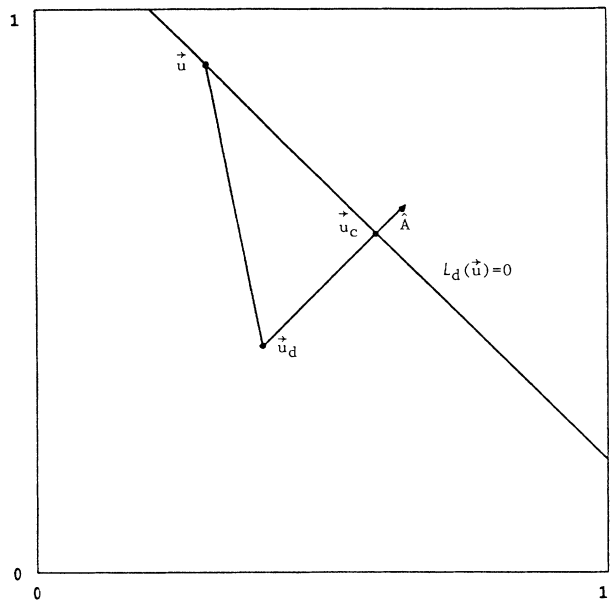

FIG. 6. The geometry of a cutting vector.

APPENDIX A: THE GEOMETRY OF A CUTTING VECTOR

The illustration in Fig. 6 depicts a DIP point $\mathbf{u}_d$ and its associated cutting line corresponding to the equality in Eq. (1.12) with $m_s=2$:

$$\sum_{l=0}^{m_s}\langle(\mathcal{V}_d)_i|\hat{M}(E;m_d+i+j,l)|(\mathcal{V}_d)_j\rangle\hat{a}_l=0 \tag{A1}$$

($\mathcal{V}_d$ is the smallest eigenvector of $\mathcal{M}_d[\mathbf{u}_d]$) or

$$\mathbf{A}\cdot\boldsymbol{a}=B\ , \tag{A2a}$$

where ($l=1,2$)

$$A_l=\langle(\mathcal{V}_d)_i|\hat{M}(E;m_d+i+j,l)|(\mathcal{V}_d)_j\rangle\ , \tag{A2b}$$

and

$$B=-\langle(\mathcal{V}_d)_i|\hat{M}(E;m_d+i+j,0)|(\mathcal{V}_d)_j\rangle\ . \tag{A2c}$$

Let us denote the linear function expression appearing in Eq. (A1) by $\mathcal{L}[\boldsymbol{a}]=\mathbf{A}\cdot\boldsymbol{a}-B$. The gradient vector for $\mathcal{L}[\boldsymbol{a}]$ is $\mathbf{A}$. We will implicitly assume that $\mathcal{L}[\mathbf{u}_d]\le 0$.

The illustration in Fig. 6 shows the unit vector $\hat{\mathbf{A}}$ pointing away from the DIP point. The closest point on the cutting line to $\mathbf{u}_d$ is denoted $\mathbf{u}_c$. We see that $\mathbf{u}_c=\mathbf{u}_d+s\hat{\mathbf{A}}$, where $\mathbf{A}\cdot(\mathbf{u}_d+s\hat{\mathbf{A}})=B$, or $s=-(\mathbf{A}\cdot\mathbf{u}_d-B)/|\mathbf{A}|$. The expression appearing within the parentheses is exactly the left-hand side of Eq. (A1) evaluated at $\mathbf{u}_d$. It therefore follows that

$$\mathbf{u}_c=\mathbf{u}_d-(\mathbf{A}\cdot\mathbf{u}_d-B)\mathbf{A}/A^2\ , \tag{A3}$$

or

$$u_{c_l}=u_{d_l}-\frac{\sum_{l'=0}^{m_s}\langle(\mathcal{V}_d)_i|\hat{M}(E;m_d+i+j,l')|(\mathcal{V}_d)_j\rangle\hat{u}_{d_l}}{\sum_{l'=1}^{m_s}\langle(\mathcal{V}_d)_i|\hat{M}(E;m_d+i+j,l')|(\mathcal{V}_d)_j\rangle^2}A_l\ . \tag{A4}$$

APPENDIX B: PROOFS OF THE u-CONVEX NATURE OF F_{mn}

Let us consider the generic form of the expectation values [$u(i)=u_i$ for $1\le i\le m_s$]:

$$F_{mn}[E;u_1,\ldots,u_{m_s}]=\langle\mathcal{V}[E;u]_i|\{\hat{M}(E;m+i+j,0)+\sum_{l=1}^{m_s}\hat{M}(E;m+i+j,l)u_l\}|\mathcal{V}[E;u]_j\rangle\ . \tag{B1}$$

Repeated i,j indices denote implicit summations over $0\le i,j\le n$. The $\mathcal{V}$ vector is the smallest eigenvector for the Hankel matrix appearing within brackets. Note that $\hat{M}(E;m+i+j,0)=M(E;m+i+j,0)$.

In order to establish the u-convex nature of F_{mn} we must show that the matrix

$$-\partial_{u_i}\partial_{u_j}F_{mn}[E;u]\ge 0 \tag{B2}$$

is non-negative (i.e., all possible expectation values are non-negative). There are two proofs available. We shall present the longer first. The spatial multidimensional generalization is immediate. The only essential difference is the re-indexing of the multidimensional moments, as done in Ref. [2]. This process is problem dependent; however, the basic structure is identical to the general one space dimension case discussed here.

1. Proof 1

Firstly, the normalized nature of $\mathcal{V}$ (implicitly u dependent) guarantees that

$$\langle\partial_{u_l}\mathcal{V}|\mathcal{V}\rangle=0\ . \tag{B3}$$

Accordingly,

$$\partial_{u_l}F_{mn}=\langle\mathcal{V}[E;u]_i|\hat{M}(E;m+i+j;l)|\mathcal{V}[E;u]_j\rangle \tag{B4}$$

and

$$\partial_{u_{l_1}}\partial_{u_{l_2}}F_{mn}=2\langle\partial_{u_{l_1}}\mathcal{V}[E;u]_i|\hat{M}(E;m+i+j;l_2)|\mathcal{V}[E;u]_j\rangle \tag{B5}$$

[the identity $\partial_{u_{l_1}}\partial_{u_{l_2}}F_{mn}=\partial_{u_{l_2}}\partial_{u_{l_1}}F_{mn}$ will become evident in Eq. (B8)].

The Hankel matrix in (B1) may be written as $\mathcal{M}[u]=M_0+\hat{\mathbf{M}}_1\mathbf{u}$. The eigenvector identity relation (for simplicity we drop the indices: $F_{mn}[u]=F[u]$)

$$(M_0+\hat{\mathbf{M}}_1\mathbf{u})|V[u]\rangle=F[u]|V[u]\rangle \tag{B6}$$

may be partially differentiated with respect to u_{l_2} yielding

$$\hat{M}(E;m+i+j,l_2)|\mathcal{V}\rangle+\mathcal{M}[u]|\partial_{u_{l_2}}\mathcal{V}\rangle$$
$$=(\partial_{u_{l_2}}F)|\mathcal{V}\rangle+F|\partial_{u_{l_2}}\mathcal{V}\rangle\ . \tag{B7}$$

Applying $\langle\partial u_{l_1}\mathcal{V}|$ to Eq. (B7) and using Eq. (B3):

$$\langle\partial_{u_{l_1}}\mathcal{V}|\hat{M}(E;m,l_2)|\mathcal{V}\rangle$$
$$=F\langle\partial_{u_{l_1}}\mathcal{V}|\partial_{u_{l_2}}\mathcal{V}\rangle-\langle\partial_{u_{l_1}}\mathcal{V}|\mathcal{M}[u]|\partial_{u_{l_2}}\mathcal{V}\rangle\ . \tag{B8}$$

We readily recognize the left-hand side of (B8) as the second-order expression $\frac{1}{2}\partial_{u_{l_1}}\partial_{u_{l_2}}F_{mn}$ given in (B5). Let $\mathbf{w}$ be an arbitrary vector. The quadratic form

$$\sum_{l_1=1}^{m_s}\sum_{l_2=1}^{m_s}w_{l_1}[\partial_{u_{l_1}}\partial_{u_{l_2}}F]w_{l_2}$$
$$=2\{F\langle\mathbf{w}\cdot\nabla\mathcal{V}|\mathbf{w}\cdot\nabla\mathcal{V}\rangle-\langle\mathbf{w}\cdot\nabla\mathcal{V}|\mathcal{M}[u]|\mathbf{w}\cdot\nabla\mathcal{V}\rangle\} \tag{B9}$$

must be negative or zero (if there is degeneracy with respect to the F eigenvalue) because

$$\frac{\langle\mathbf{w}\cdot\nabla\mathcal{V}|\mathcal{M}[u]|\mathbf{w}\cdot\nabla\mathcal{V}\rangle}{\langle\mathbf{w}\cdot\nabla\mathcal{V}|\mathbf{w}\cdot\nabla\mathcal{V}\rangle}\geq F\ . \tag{B10}$$

(Recall, $|\mathcal{V}\rangle$ is the eigenvector for the smallest eigenvalue of $\mathcal{M}[u]$.) This is true for any w vector; therefore Eq. (B2) holds.

2. Proof 2

The function $F_{mn}[u]$ is convex if in a neighborhood of an arbitrary point u_a we have

$$F_{mn}[u_a]+\sum_l\delta u_l\partial_{u_l}F_{mn}[u_a]\geq F_{mn}[u_a+\delta u]\ . \tag{B11}$$

From Eq. (B4) it follows that the above condition becomes ($\mathcal{V}_a=\mathcal{V}[u_a]$, while $\mathcal{V}[u_a+\delta u]=\mathcal{V}$)

$$\langle\mathcal{V}_a|\mathcal{M}[u_a]|\mathcal{V}_a\rangle+\sum_l\delta u_l\langle\mathcal{V}_a|\hat{M}_l|\mathcal{V}_a\rangle$$
$$\geq\langle\mathcal{V}|\mathcal{M}[u_a+\delta u]|\mathcal{V}\rangle\ .$$

However, Eq. (B12) is always valid because the left-hand side is simply $\langle\mathcal{V}_a|\mathcal{M}[u_a+\delta u]|\mathcal{V}_a\rangle$ and is always greater than or equal to $\langle\mathcal{V}|\mathcal{M}[u_a+\delta u]|\mathcal{V}\rangle$ (i.e., $\mathcal{V}[u]$ is the eigenvector for the smallest eigenvalue of $\mathcal{M}[u]$).

[1] A. Weinstein, Mem. Sci. Math. No. 88 (1937); P. O. Lowdin, Phys. Rev. **139**, A357 (1965); M. F. Barnsley, J. Phys. A **11**, 55 (1978).

[2] C. R. Handy, D. Bessis, G. Sigismondi, and T. D. Morley, Phys. Rev. Lett. **60**, 253 (1988).

[3] C. R. Handy and P. Lee, J. Phys. A **24**, 1565 (1991).

[4] C. R. Handy, D. Bessis, and T. D. Morley, Phys. Rev. A **37**, 4557 (1988).

[5] V. Chvatal, *Linear Programming* (Freeman, New York, 1983).

[6] C. R. Handy and D. Bessis, Phys. Rev. Lett. **55**, 931 (1985); C. R. Handy, J. Phys. A **18**, 3593 (1985); D. Bessis, E. R. Vrscay, and C. R. Handy, *ibid.* **20**, 419 (1987); C. R. Handy and R. M. Williams, *ibid.* **20**, 2315 (1987).

[7] J. A. Shohat and J. D. Tamarkin, *The Problem of Moments* (American Mathematical Society, Providence, RI, 1963).

[8] M. Reed and B. Simon, *Methods of Modern Mathematical Physics* (Academic, New York, 1978).

[9] F. T. Hioe, D. MacMillen, and E. W. Montroll, J. Math. Phys. **17**, 1320 (1976).